Supporting information for

Size-dependent catalytic reactivity of NO reduction by CO mediated by the $Rh_nV_2O_3^-$ clusters (n = 2–5)

Jin-You Chen,[a] Hai Zhu,[b] Tong-Mei Ma,*[,a] Xiao-Na Li*[,b]

[a] China School of Chemistry and Chemical Engineering, South China University of Technology, 381 Wushan Road, Tianhe District, Guangzhou 510641, P. R. China

[b] School of Chemistry and Chemical Engineering, Beijing Institute of Technology, Beijing 102488, P. R. China

Corresponding Authors:

*Tong-Mei Ma: tongmei@scut.edu.cn; Xiao-Na Li: xiaonali@bit.edu.cn

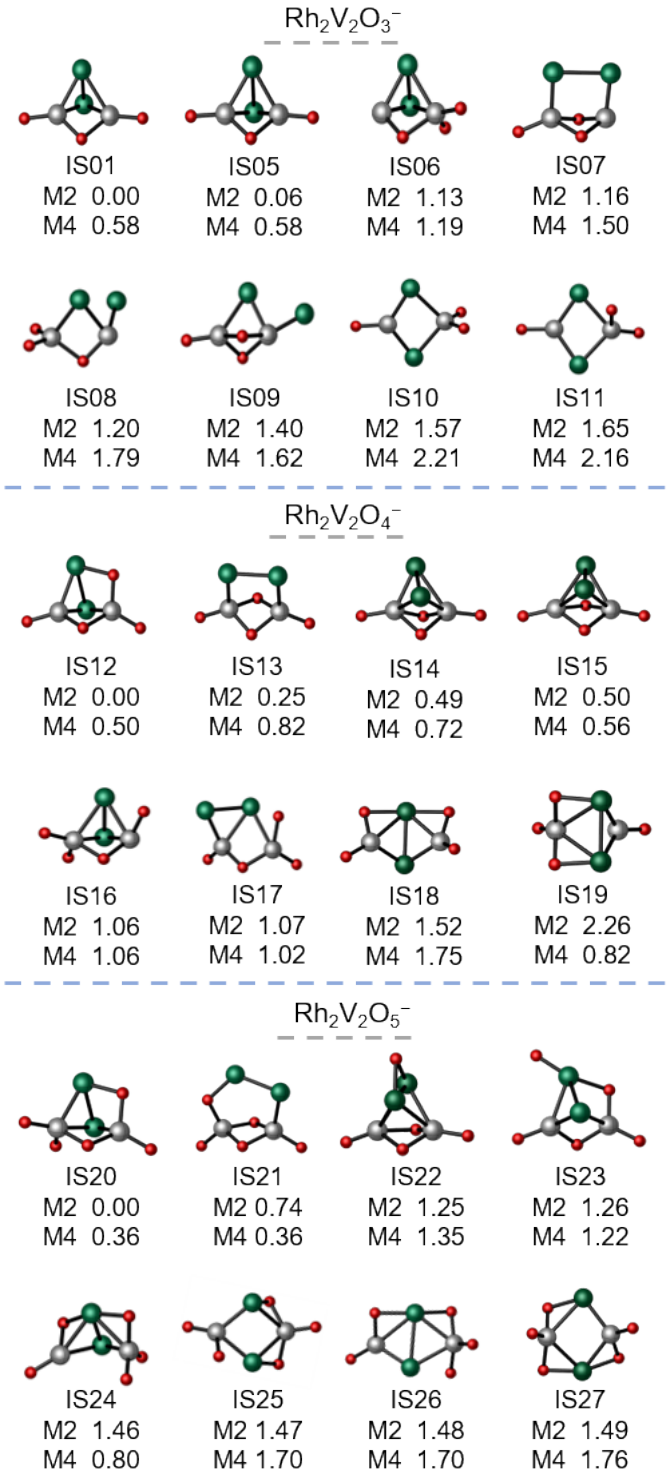

Figure S1. The DFT calculated isomers of $Rh_2V_2O_{3-5}^-$. The zero-point vibration corrected energies (ΔH_0, eV) are given. Mx (x = 2 and 4) represents different spin multiplicities.

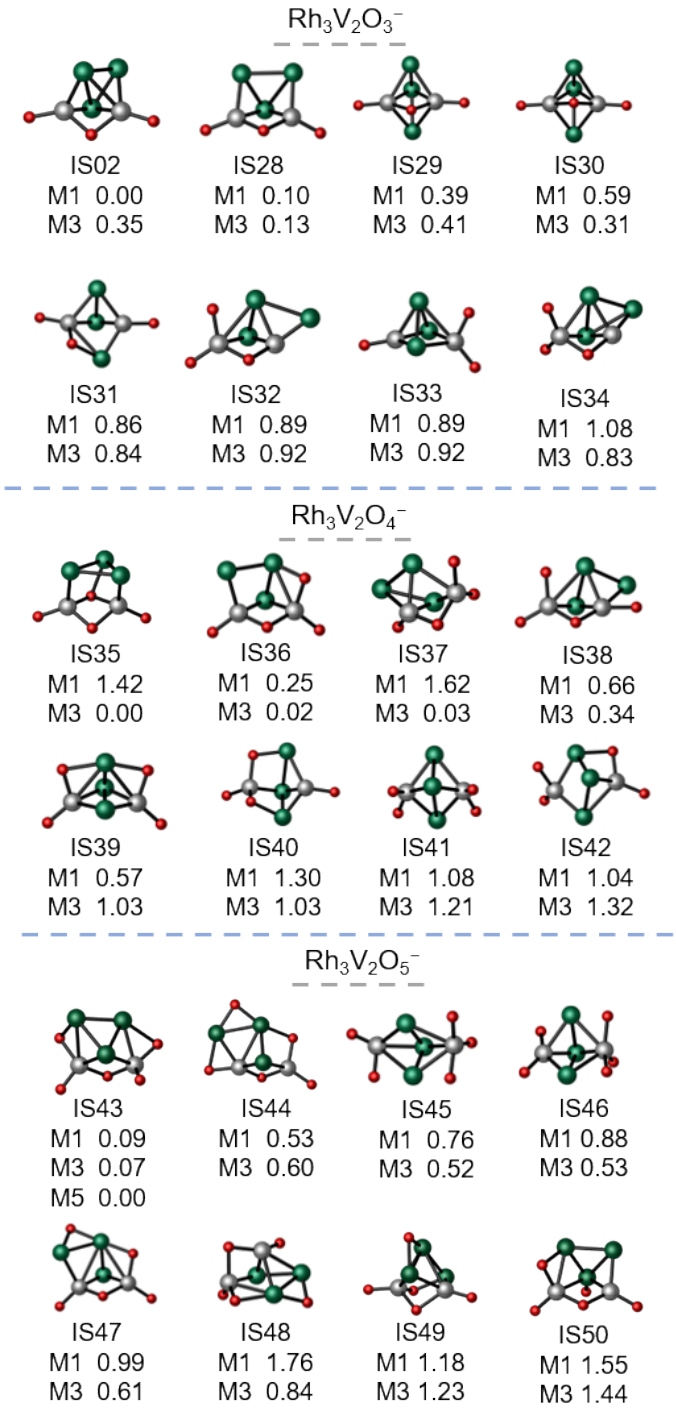

Figure S2. The DFT calculated isomers of $Rh_3V_2O_{3–5}^-$. The zero-point vibration corrected energies (ΔH_0, eV) are given. Mx (x = 1, 3, and 5) represents different spin multiplicities.

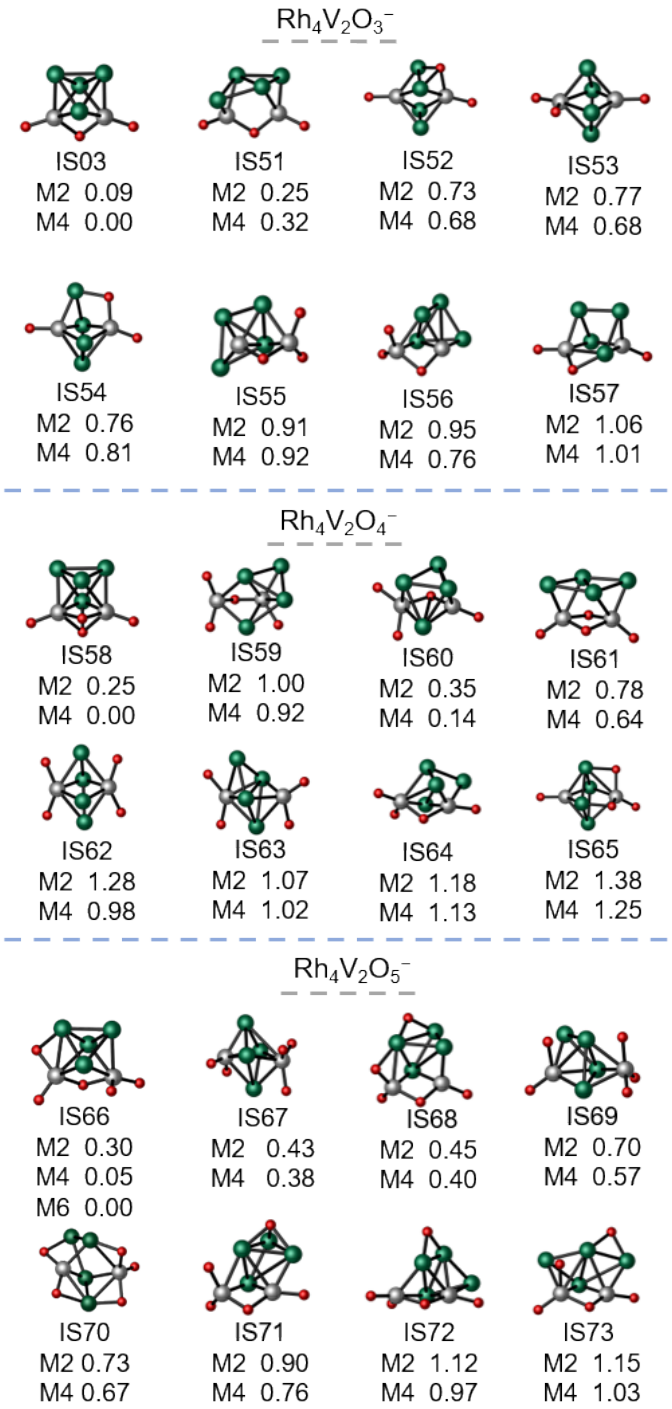

Figure S3. The DFT calculated isomers of $Rh_4V_2O_{3-5}^-$. The zero-point vibration corrected energies (ΔH_0, eV) are given. Mx (x = 2, 4, and 6) represents different spin multiplicities.

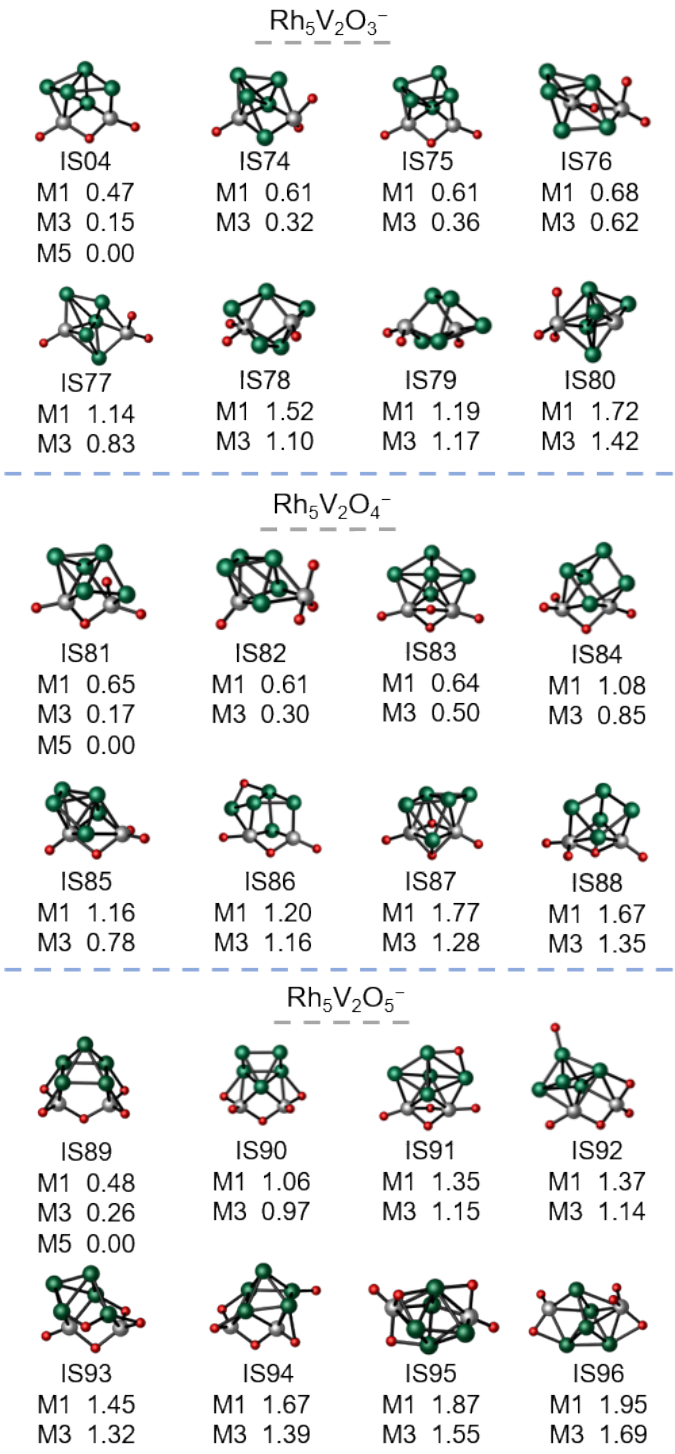

Figure S4. The DFT calculated isomers of $Rh_5V_2O_{3–5}^-$. The zero-point vibration corrected energies (ΔH_0, eV) are given. Mx (x = 1, 3, and 5) represents different spin multiplicities.

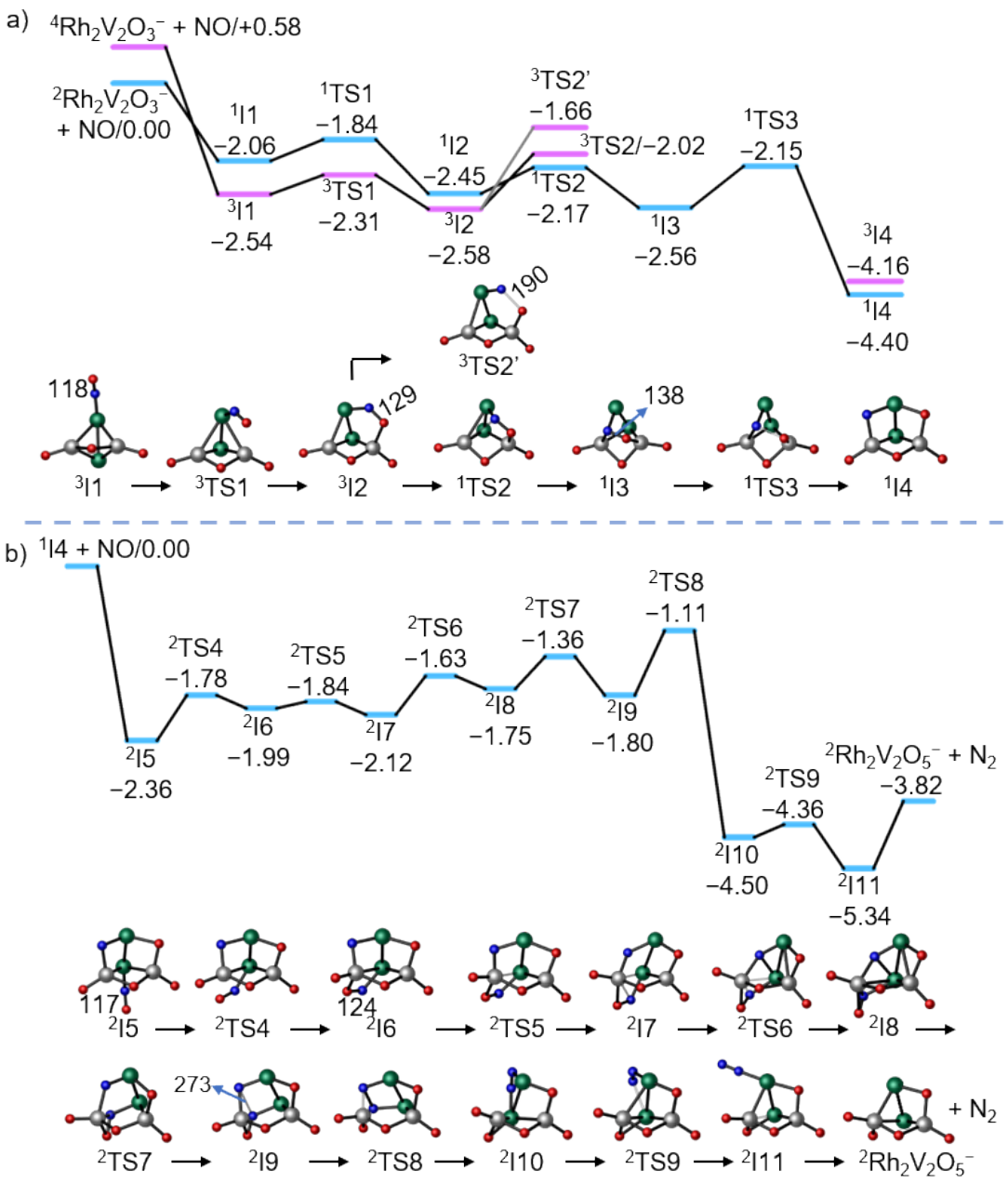

Figure S5. The DFT calculated potential energy profile for the reaction $Rh_2V_2O_3^-$ + 2NO (a, b). Relative energies (ΔH_0, eV) for Is and TSs are shown. Bond lengths are given in pm.

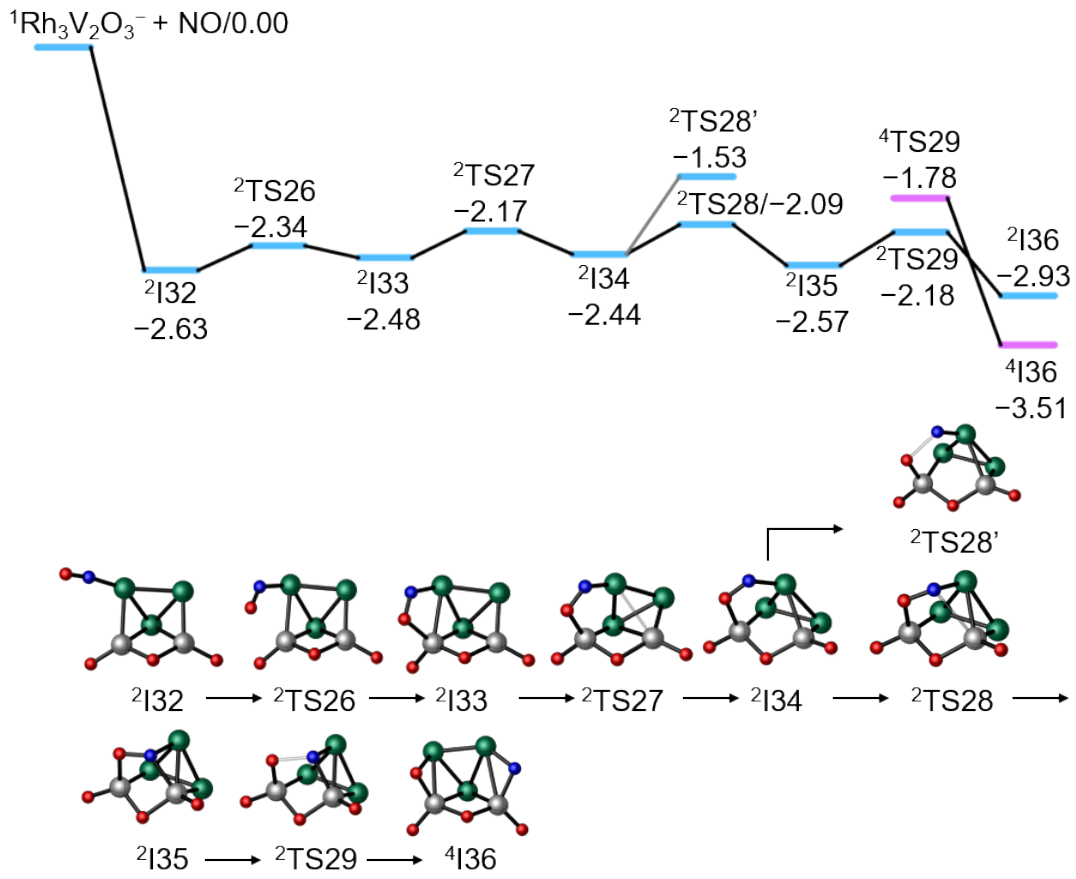

Figure S6. The DFT-calculated potential energy of profile for reaction $Rh_3V_2O_3^-$ + NO. Relative energies (ΔH_0, eV) are for Is and TSs are shown.

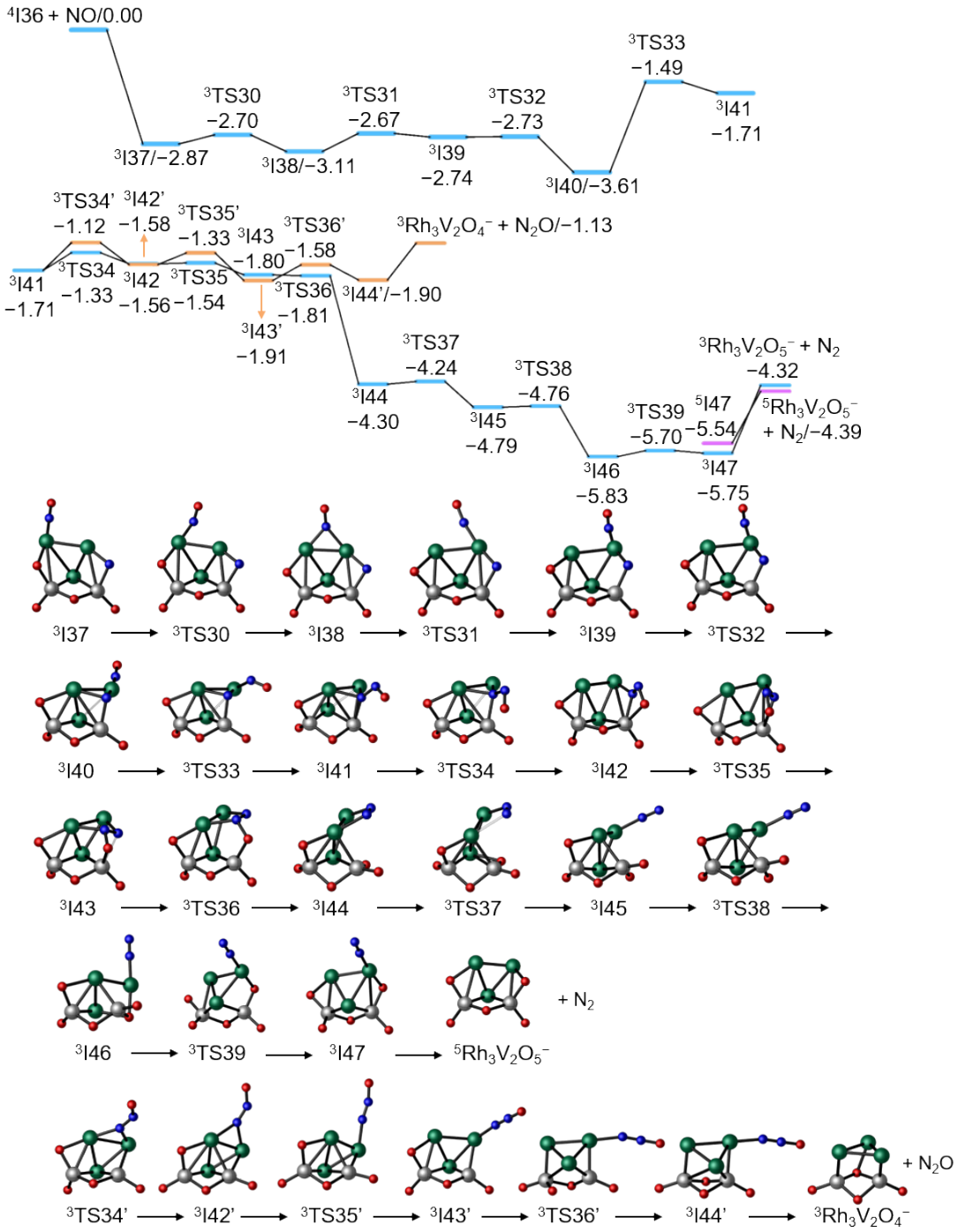

Figure S7. The DFT-calculated potential energy of profile for reaction $Rh_3V_2O_3NO^-$ + NO. Relative energies (ΔH_0, eV) are for Is and TSs are shown.

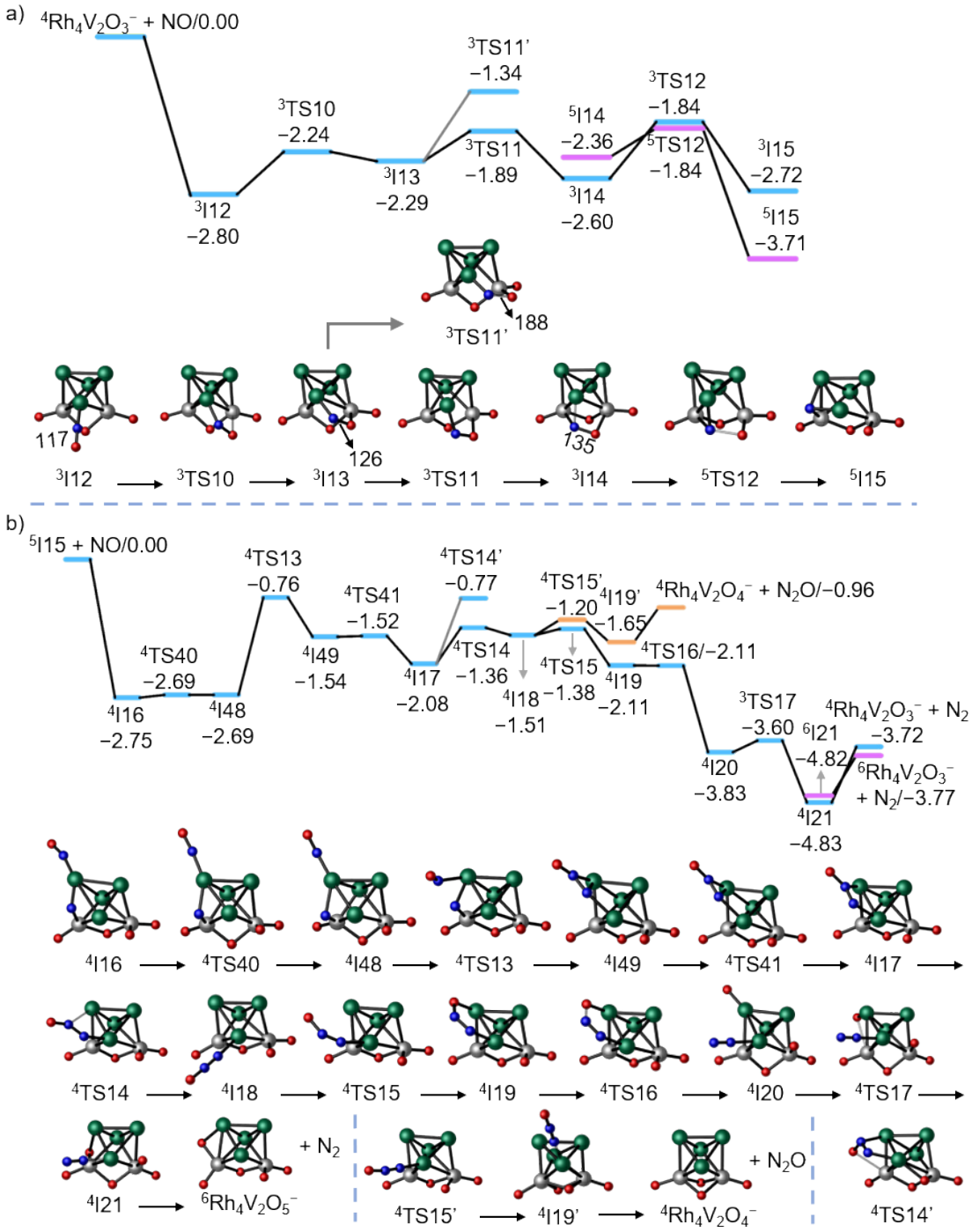

Figure S8. The DFT-calculated potential energy of profile for reaction $Rh_4V_2O_3^-$ + 2NO. Relative energies (ΔH_0, eV) are for Is and TSs are shown. Bond lengths are given in pm.

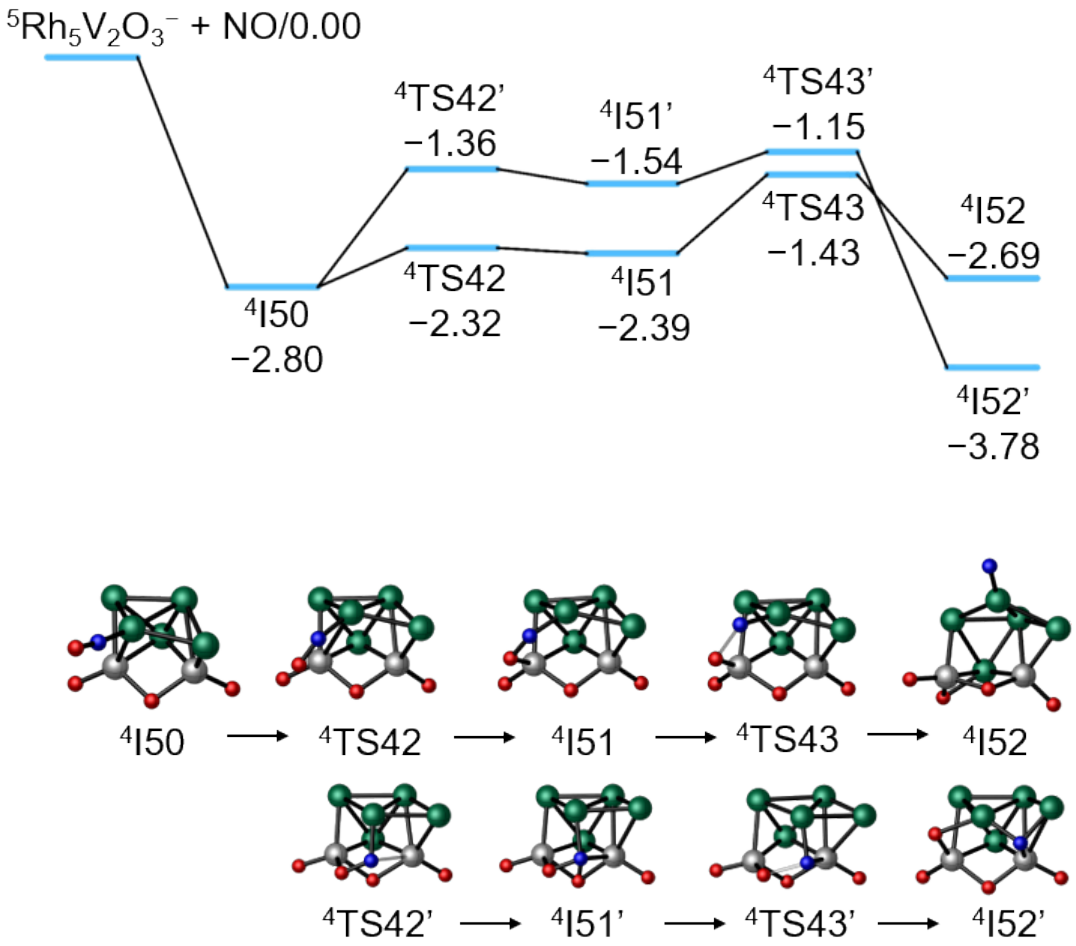

Figure S9. The DFT-calculated potential energy of profile for reaction $Rh_5V_2O_3^-$ + NO. Relative energies (ΔH_0, eV) are for Is and TSs are shown.

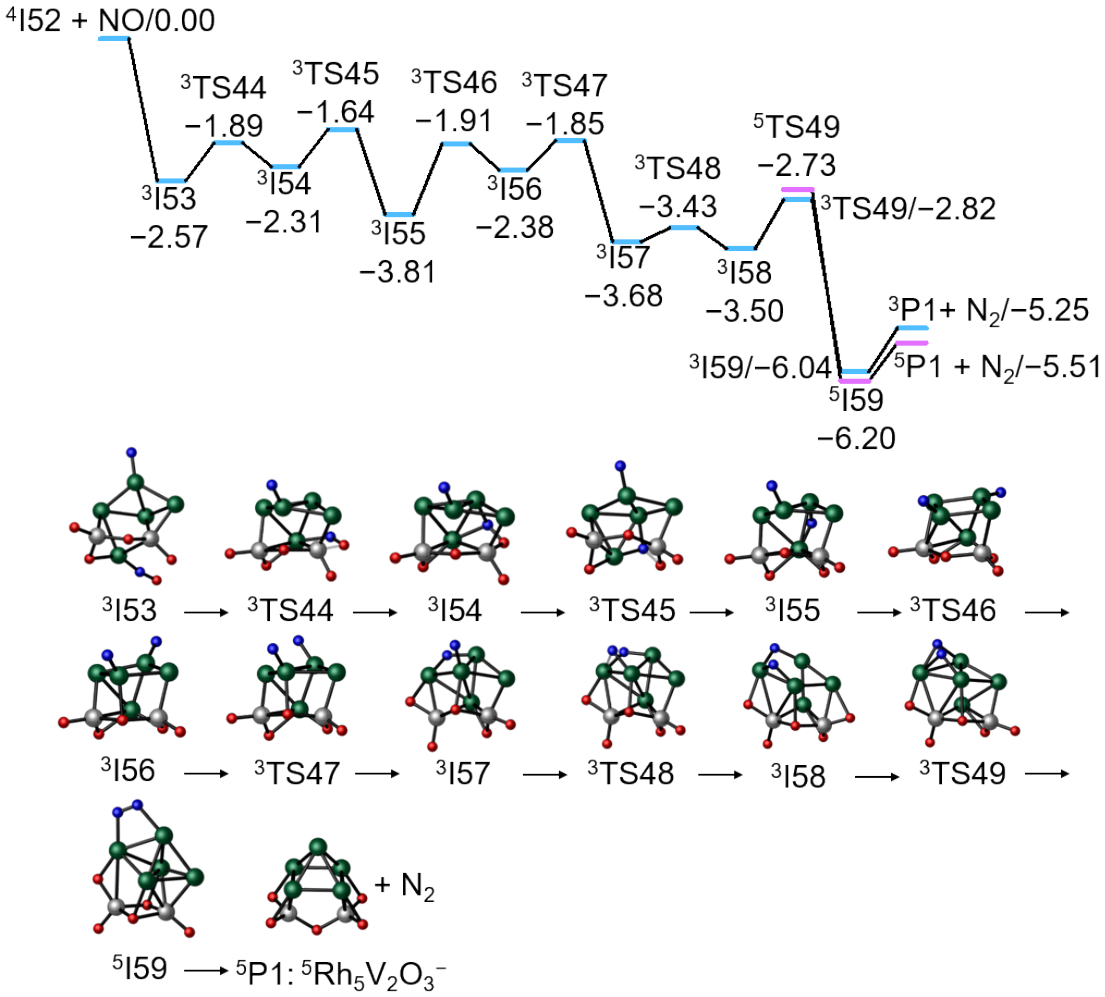

Figure S10. The DFT-calculated potential energy of profile for reaction $Rh_5V_2O_3NO^-$ + NO. Relative energies (ΔH_0, eV) are for Is and TSs are shown.

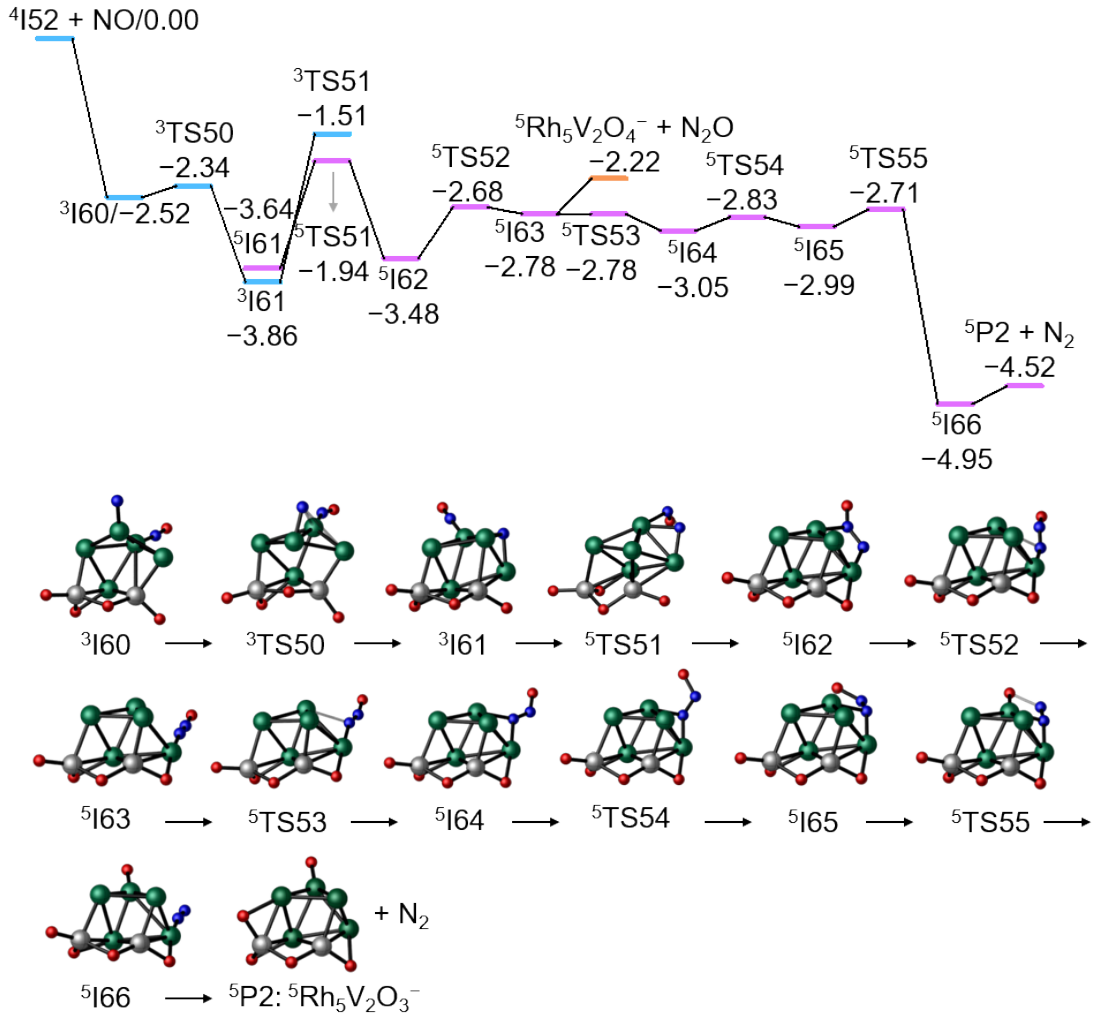

Figure S11. The DFT-calculated potential energy of profile for reaction $Rh_5V_2O_3NO^-$ + NO. Relative energies (ΔH_0, eV) are for Is and TSs are shown.

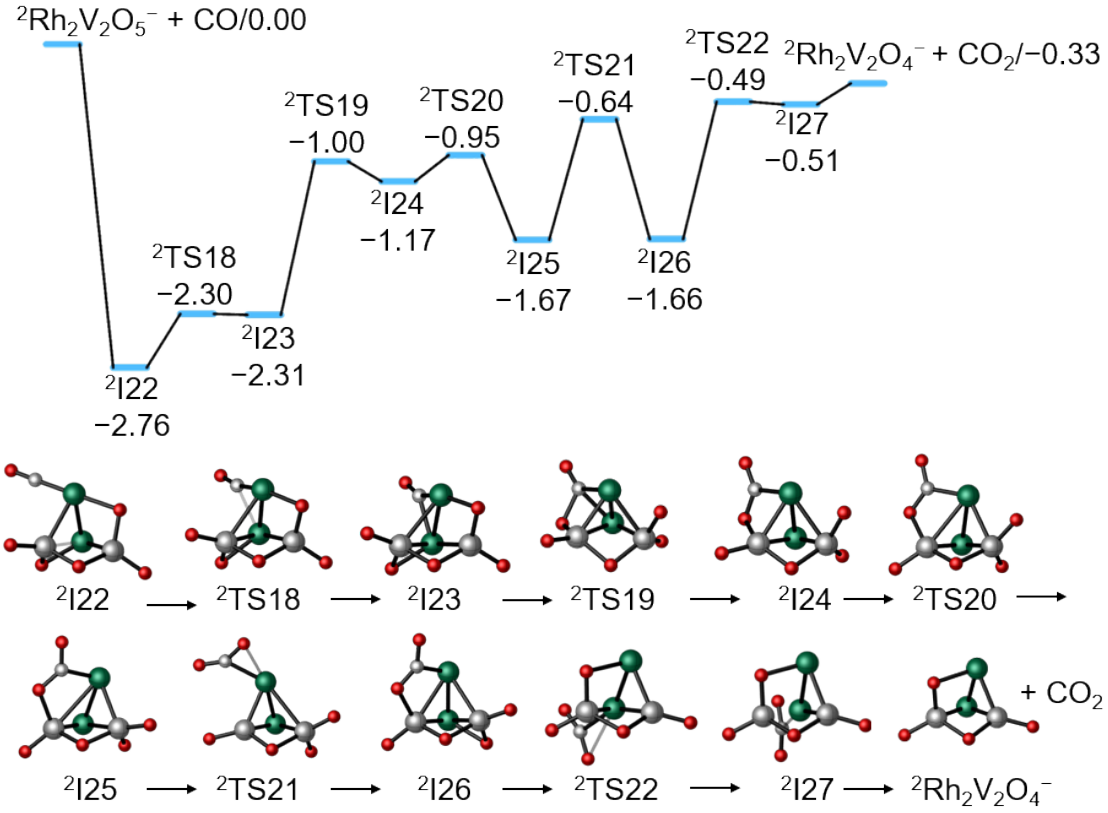

Figure S12. The DFT-calculated potential energy of profile for reaction $Rh_2V_2O_5^-$ + CO. Relative energies (ΔH_0, eV) are for Is and TSs are shown.

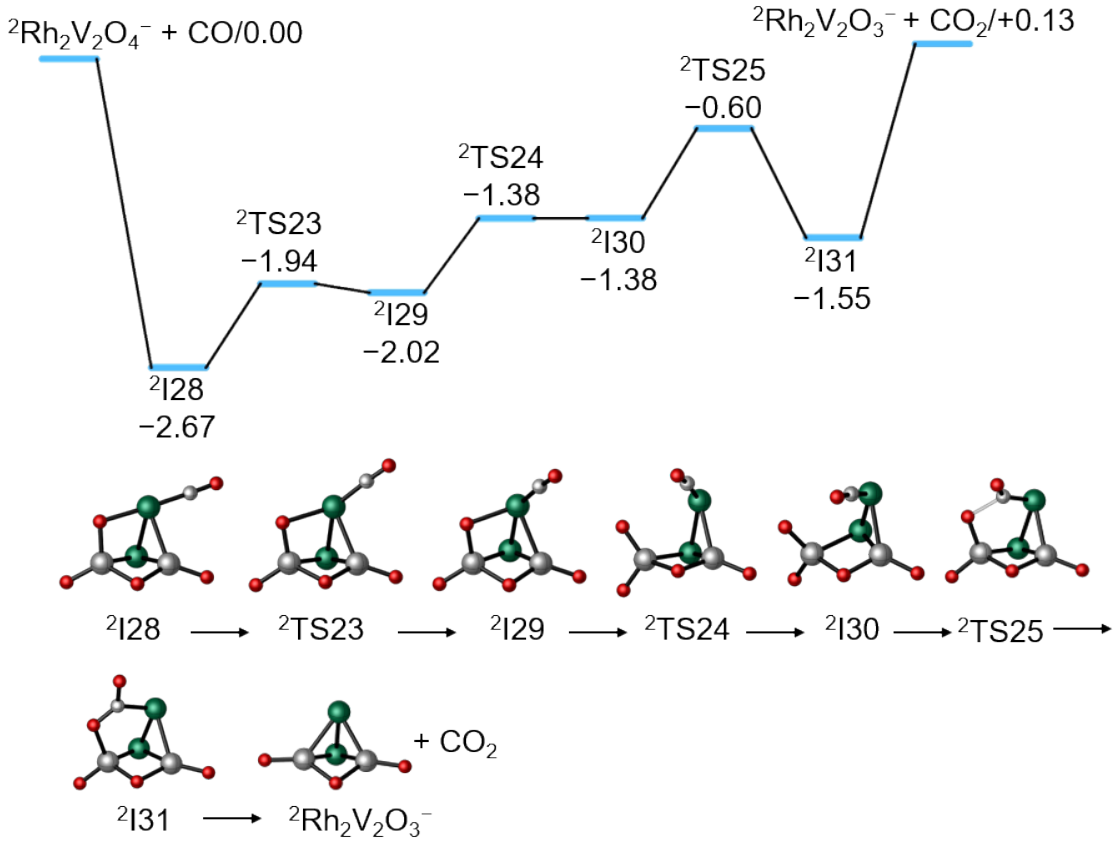

Figure S13. The DFT-calculated potential energy of profile for reaction $Rh_2V_2O_4^-$ + CO. Relative energies (ΔH_0, eV) are for Is and TSs are shown.

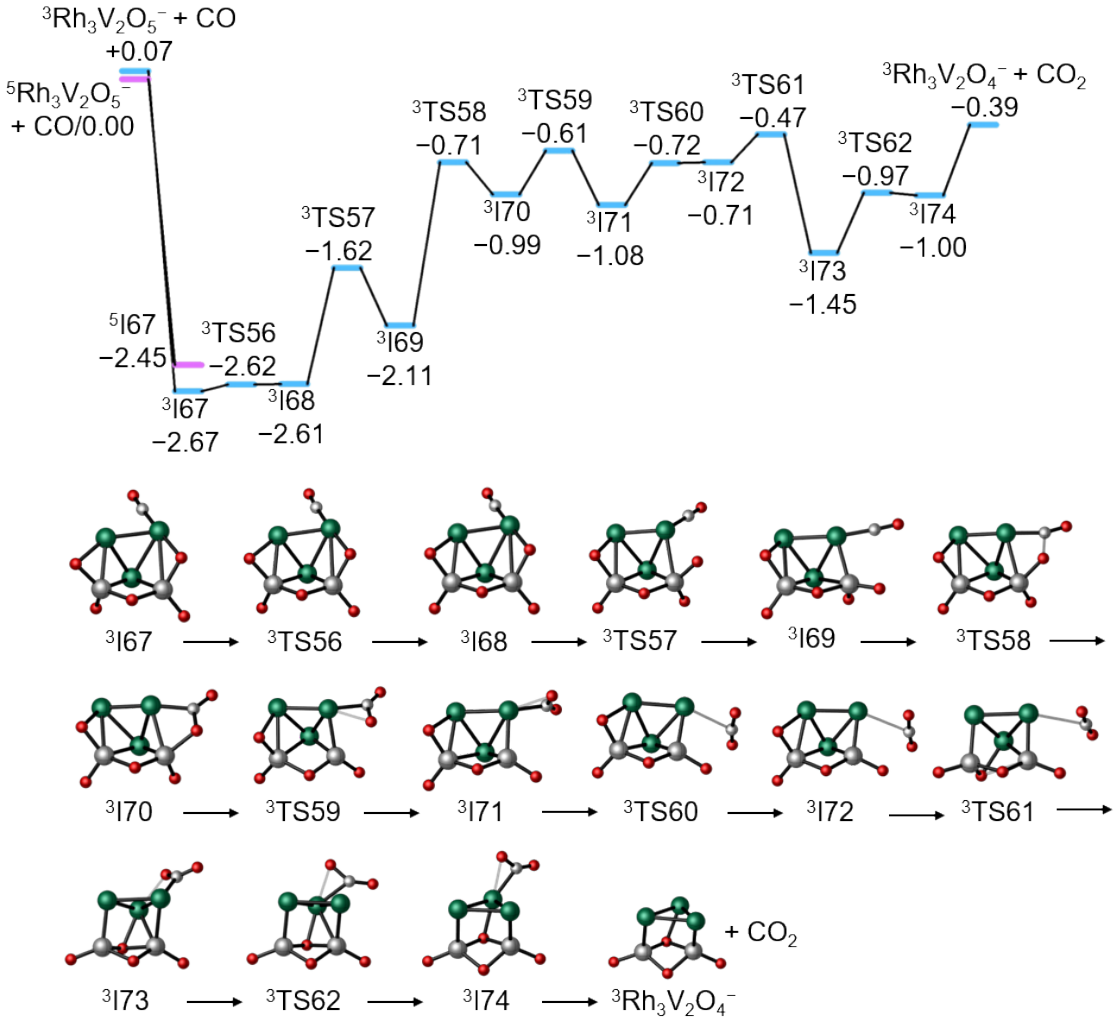

Figure S14. The DFT-calculated potential energy of profile for reaction $Rh_3V_2O_5^-$ + CO. Relative energies (ΔH_0, eV) are for Is and TSs are shown.

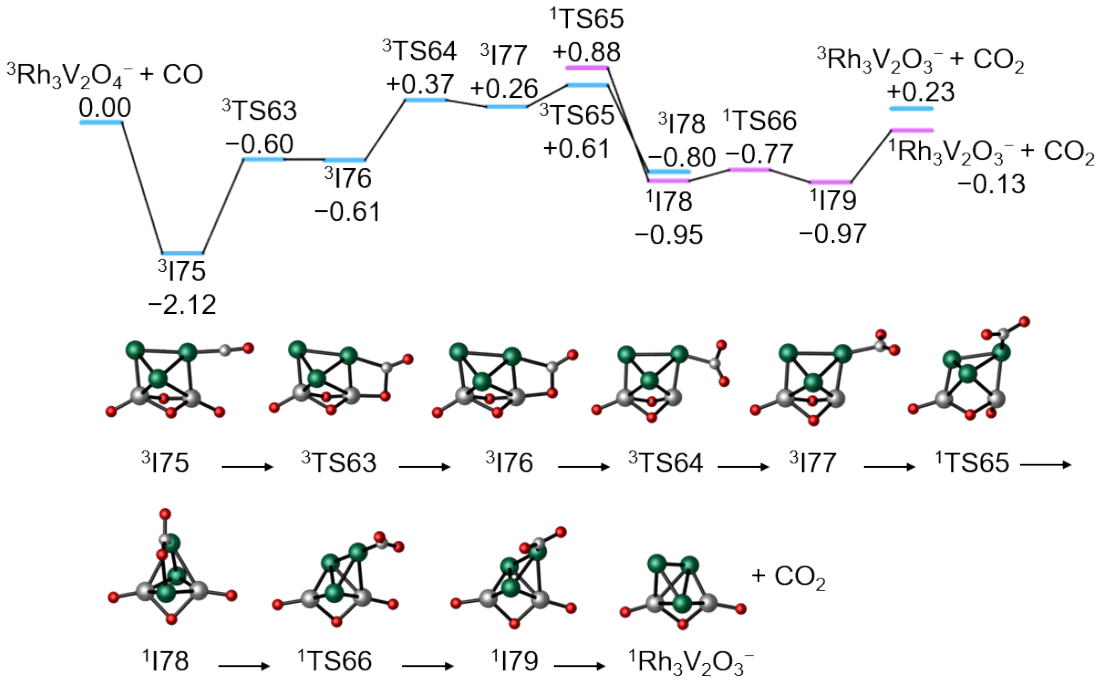

Figure S15. The DFT-calculated potential energy of profile for reaction $Rh_3V_2O_4^-$ + CO. Relative energies (ΔH_0, eV) are for Is and TSs are shown.

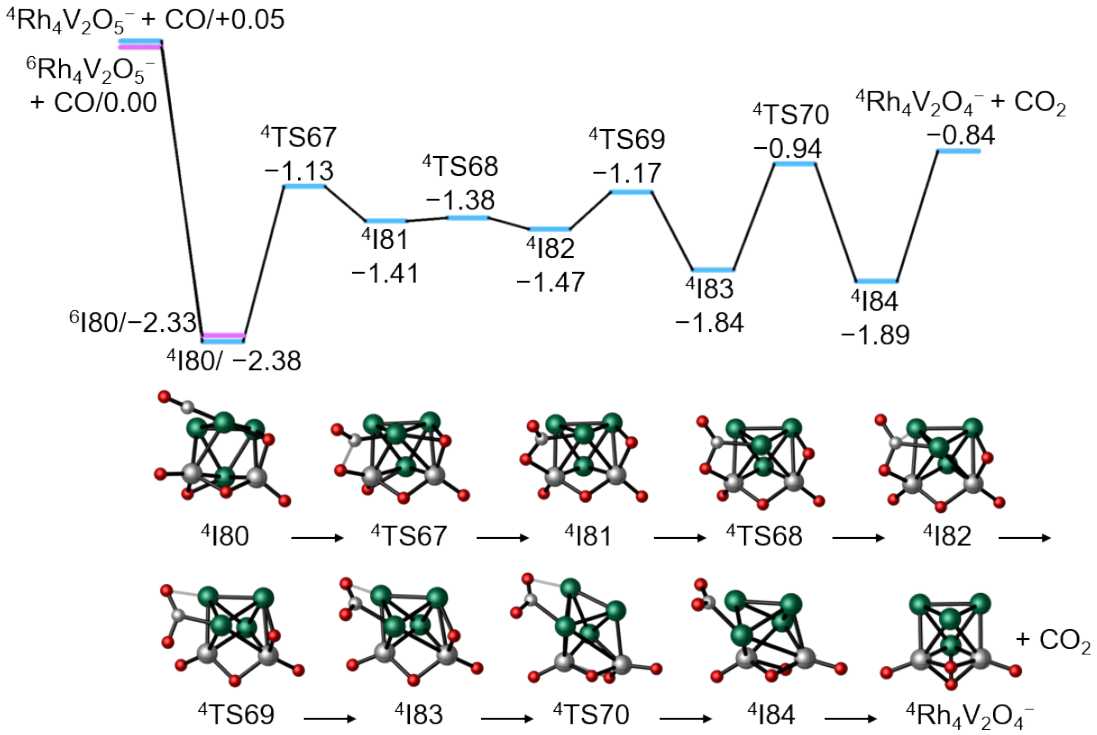

Figure S16. The DFT-calculated potential energy of profile for reaction $Rh_4V_2O_5^-$ + CO. Relative energies (ΔH_0, eV) are for Is and TSs are shown.

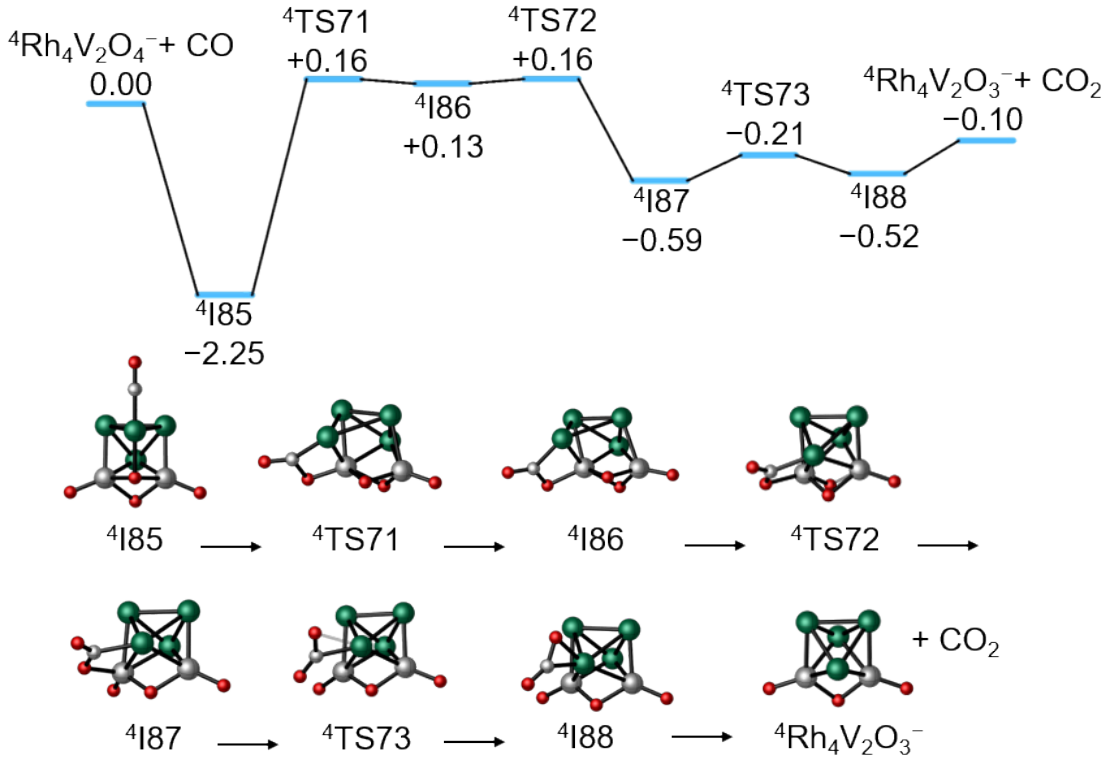

Figure S17. The DFT-calculated potential energy of profile for reaction $Rh_4V_2O_4^-$ + CO. Relative energies (ΔH_0, eV) are for Is and TSs are shown.

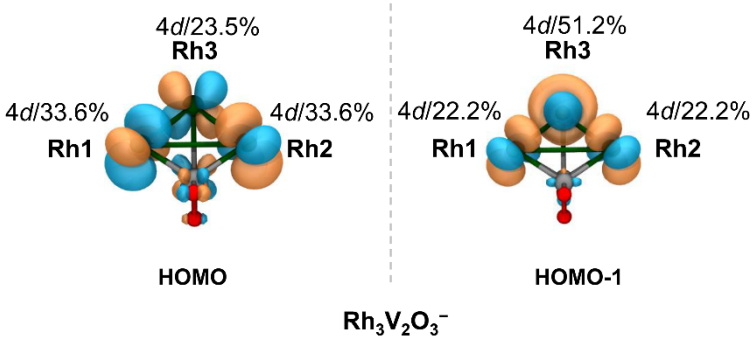

Figure S19. The HOMO and HOMO-1 of $Rh_3V_2O_3^-$.

Methods

The DFT calculations with M06L[1] functional by using the Gaussian 09[2] program were carried out to investigate the structures of $Rh_nV_2O_3^-$ (n = 2–5) and the mechanisms on the reactions of $Rh_nV_2O_3^-$ (n = 2–5) with NO and $Rh_nV_2O_{4-5}^-$ (n = 2–4) with CO. For all the calculations, the polarized split-valence basis set TZVP[3,4] for V, N, C, O, and the Stuttgart/Dresden relativistic effective core potentials (denoted as SDD in Gaussian software)[5] for Rh atom were adopted. In mechanism calculations, reaction intermediates (Is) and transition states (TSs) were optimized. The TSs were optimized by using the Berny algorithm method[6] and its initial guess structures were obtained by relaxed potential energy surface scans using single or multiple internal coordinates. In order to verify that each TS connects the appropriate local minima, intrinsic reaction coordinate calculations were used.[7] Vibrational frequency calculations were performed to confirm that Is have zero and TSs have only one imaginary frequency, respectively. The zero-point vibrational corrected energies at T = 0 K (ΔH_0 in eV) were reported in this work. The electrostatic potential (ESP) maps and the spin populations of V_2O_3 and $Rh_nV_2O_3^-$ (n = 2−5), and the selected molecular orbitals of $Rh_nV_2O_3^-$ (n = 2−5), $Rh_nV_2O_3(NO)^-$ (n = 2−5) and $Rh_nV_2O_3(NO)_2^-$ (n = 2−5) were performed by using the Multiwfn program[8] and were drawn by the Visual Molecular Dynamics program.[9]

References

1 Zhao, Y.; Truhlar, D. G. *J. Chem. Phys.*, 2006, **125**, 194101.

2 M. J. Frisch, G. W. Trucks, H. B. Schlegel, G. E. Scuseria, M. A. Robb, J. R. Cheeseman, G. Scalmani, V. Barone, B. Mennucci, G. A. Petersson, H. Nakatsuji, M. Caricato, X. Li, H. P. Hratchian, A. F. Izmaylov, J. Bloino, G. Zheng, J. L. Sonnenberg, M. Hada, M. Ehara, K. Toyota, R. Fukuda, J. Hasegawa, M. Ishida, T. Nakajima, Y. Honda, O. Kitao, H. Nakai, T. Vreven, J. A. Montgomery, Jr., J. E. Peralta, F. Ogliaro, M. Bearpark, J. J. Heyd, E. Brothers, K. N. Kudin, V. N. Staroverov, T. Keith, R. Kobayashi, J. Normand, K. Raghavachari, A. Rendell, J. C. Burant, S. S. Iyengar, J. Tomasi, M. Cossi, N. Rega, J. M. Millam, M. Klene, J. E. Knox, J. B. Cross, V. Bakken, C. Adamo, J. Jaramillo, R. Gomperts, R. E. Stratmann, O. Yazyev, A. J. Austin, R. Cammi, C. Pomelli, J. W. Ochterski, R. L. Martin, K. Morokuma, V. G. Zakrzewski, G. A. Voth, P. Salvador, J. J. Dannenberg, S. Dapprich, A. D. Daniels, O. Farkas, J. B. Foresman, J. V. Ortiz, J. Cioslowski, and D. J. Fox, *Gaussian 09*, revision D.01, Gaussian, Inc., Wallingford CT, 2013.

3 R. Krishnan, J. S. Binkley, R. Seeger and J. A. Pople, *J. Chem. Phys.*, 1980, **72**, 650–654.

4 W. J. Hehre, R. Ditchfield and J. A. Pople, *J. Chem. Phys.*, 1972, **56**, 2257–2261.

5 M. Dolg, H. Stoll and H. Preuss, *J. Chem. Phys.*, 1989, **90**, 1730–1734.

6 H. B. Schlegel, *J. Comput. Chem.*, 1982, **3**, 214–218.

7 C. Gonzalez and H. B. Schlegel, *J. Chem. Phys.*, 1989, **90**, 2154–2161.

8 T. Lu and F. Chen, *J. Comput. Chem.*, 2012, **33**, 580–592.

9 W. Humphrey, A. Dalke and K. Schulten, *J. Mol. Graph.*, 1996, **14**, 33–38.